Scientific Research Publishing

Advances in Molecular Imaging, 2017, 7, 1-11
http://www.scirp.org/journal/ami
ISSN Online: 2161-6752
ISSN Print: 2161-6728

High-Uptake Areas on ^{18}F-FRP170 PET Image Necessarily Include Proliferating Areas in Glioblastoma: A Superimposed Image Study Combining ^{18}F-FRP170 PET with ^{11}C-methionine PET

Takaaki Beppu[1], Toshiaki Sasaki[2], Yuichi Sato[1], Kazunori Terasaki[2]

[1]Department of Neurosurgery, Iwate Medical University, Morioka, Japan
[2]Cyclotron Research Center, Iwate Medical University, Morioka, Japan
Email: tbeppu@iwate-med.ac.jp

How to cite this paper: Beppu, T., Sasaki, T., Sato, Y. and Terasaki, K. (2017) High-Uptake Areas on ^{18}F-FRP170 PET Image Necessarily Include Proliferating Areas in Glioblastoma: A Superimposed Image Study Combining ^{18}F-FRP170 PET with ^{11}C-methionine PET. *Advances in Molecular Imaging*, **7**, 1-11.
https://doi.org/10.4236/ami.2017.71001

Received: February 20, 2017
Accepted: March 20, 2017
Published: March 23, 2017

Abstract

Areas of uptake on positron emission tomography with 1-(2-[^{18}F]fluoro-1-[hydroxymethyl]ethoxy)methyl-2-nitroimidazole (FRP170 PET), a hypoxic cell radiotracer, can include regions retaining highly proliferative activity despite tissue hypoxia. The aim of this study was to clarify whether FRP170 image can detect densely populated hypoxic areas without proliferating potential in glioblastoma. We performed FRP170 PET scan and L-methyl-^{11}C-methionine (MET) PET scan in eight patients with non-treated glioblastoma. Standardized uptake values (SUVs) within tumor and apparent normal brain were measured on each FRP170 and MET image for all patients. To visualize actively proliferative areas on MET image we initially extracted pixels showing a ratio of SUV in tumor to SUV in normal brain (T/N) > 1.6. For FRP170 image, we changed the thresholds between minimum SUV and maximum SUV in tumor. Pixels showing SUV above each threshold were extracted and superimposed on previously extracted pixels from MET image. We estimated whether pixels extracted with MET and FRP170 were visually separated on superimposed image for each patient. When no threshold was established, uptake areas on MET image and FRP170 image overlapped widely on superimposed image in all patients. The higher threshold for FRP170 image diminished FRP170-extracted pixels, and shrunk overlapped areas on superimposed image. However, pixels extracted from FRP170 images could not be completely separated from pixels extracted from MET images in all patients, even with threshold raised to almost maximum SUV. The current findings suggest that uptake areas on FRP170 PET scan necessarily include proliferating areas in glioblastoma.

Keywords

^{18}F-FRP170 PET, ^{11}C-MET PET, Hypoxia, Proliferation, Glioblastoma

1. Introduction

Although therapeutic technologies have been advancing rapidly, glioblastoma still shows the poorest prognosis of the malignant brain tumors. Most malignant tumors including glioblastoma retain a hypoxic condition offering a crucial means of determining the biological characteristics of the tumor. Indeed, malignant tumors take advantage of hypoxia to induce neovascularization, gene instability, and resistance to therapy. Visual assessment of hypoxia is thus worthwhile for diagnosis and treatment in patients with glioblastoma. Positron emission tomography (PET) using hypoxic cell tracers offers an attractive method for detecting hypoxic cells as a simple, minimally invasive, repeatable imaging modality not limited to superficial tumor [1]. Hypoxic cells in glioblastoma have been detected using PET with hypoxic cell tracers including [^{18}F]fluoromisonidazole (FMISO) [2] [3] and 1-(2-[^{18}F]fluoro-1-[hydroxymethyl]ethoxy)methyl-2-nitroimidazole (FRP170) [4] [5], both of which are synthesized from 2-nitroimidazole. Although FMISO became available before FRP170, FRP170 is considered superior in terms of fine contrast, rapid clearance from blood, and short period from tracer injection [4] [6]. When hypoxia is assessed within tumors on FRP170 PET imaging, the extent to which the hypoxic area retains proliferative activity offers an essential means for clarifying the biological characteristics of lesions. Theoretically, hypoxia is expected to correlate inversely with proliferative activity, since cell hypoxia within a tumor primarily causes excessive oxygen consumption due to cell proliferation [7] [8]. However, immunohistochemical studies using Ki-67 staining on specimens obtained from tracer-accumulating areas have revealed that areas of FRP170 and FMISO accumulation retain highly proliferative activity despite tissue hypoxia [9] [10] [11]. We hypothesized that regions of extremely high standardized uptake value (SUV) that comprise densely populated hypoxic cells accumulating with FRP170 are supposed to include regions with ultimately far fewer proliferating cells. The aim of this study was to clarify whether FRP170 PET could detect densely populated hypoxic areas without proliferative potential, when FRP170 PET alone would be performed. To clarify the aim of this study, we evaluated each distribution of pixels of hypoxic cells or proliferating cells on superimposed images composed of FRP170 PET image and L-methyl-^{11}C-methionine (MET) PET image.

2. Patients and Methods

2.1. Patients

All study protocols were approved by the ethics committee at our institute (H22-2, H22-70). Patients recruited to this study were admitted to our institute

between April 2008 and May 2015. Inclusion criteria for the study were: ≥20 years old with untreated glioblastoma localized to the cerebral white matter other than the brainstem or cerebellum; and voluntary provision of written informed consent to participate. Glioblastoma was diagnosed based on the histological features of specimens obtained during tumor resection after the proceedings in this study. Eight patients (5 men, 3 women; age range, 36 - 75 years) were enrolled in this study. To confirm the localization of tumor in each patient, MRI was performed using a 3.0-T MRI system (Discovery MR750; GE Healthcare Japan, Tokyo, Japan) under the following sequence parameters: echo time, 110 ms; repetition time, 11,000 ms; matrix, 448 × 224 for gadolinium-enhanced T1-weighted imaging (Gd-T1WI). The location of the main tumor bulk was the frontal lobe in 4 patients, parietal lobe in 3 patients, and temporal lobe in 1 patient.

2.2. FRP170 PET and MET PET

FRP170 PET image and MET PET image were scanned on different days within the same week. FRP170 was synthesized using on-column alkaline hydrolysis per the methods described by Ishikawa *et al.* [12]. The final formulation for injection included normal saline containing 2.5% v/v ethanol using solid-phase extraction techniques. Sixty minutes after intravenous injection of approximately 370 MBq (mean dose, 5.5 MBq/kg) of FRP170, PET scan was performed using a PET/computed tomography system (Eminence Sophia SET3000 GCT/M; Shimadzu, Japan). PET images were reconstructed using Fourier rebinning plus ordered subset expectation maximization with 4 iterations and 26 subsets, under the following conditions: field of view, 256 mm^2; matrix, 128 × 128; pixel size, 2.0 × 2.0 mm^2; and slice sickness, 2.6 mm.

MET was prepared using the solid-phase ^{11}C-methylation method with $[^{11}C]CH_3I$ as reported previously [13]. In brief, $[^{11}C]CH_3I$ was bound to a Sep-Pak tC18 Plus cartridge (Waters, Milford, MA) loaded with a solution of L-homocysteine thiolactone. The cartridge was then eluted with 0.5% acetic acid. After evaporating the solution, the residue was dissolved in physiological saline. The radiochemical purity of the produced MET was >99%. At 30 min after intravenous injection of MET with a dose of 325 - 398 MBq (mean, 6.5 MBq/kg), PET scan was performed using the same equipment and procedures as those for FRP170 PET.

On scanned color images, regions of interest (ROIs) 6 mm in diameter were placed on the high uptake areas within the tumor and in apparently normal cerebral white matter of the contralateral side, in accordance with a previous report [14]. After inputting data of patient's body weight (g) and injected dose of tracer (MBq) into an analyzing software equipped in a PET/computed tomography system, the minimum SUV (SUVmin), maximum SUV (SUVmax), and average SUV (SUVavg) in the ROI within the tumor were automatically calculated for each scan of each patient. In apparently normal brain, SUVavg alone was measured as the absolute value. T/N ratio was calculated as a SUV value

considered to represent tumor divided by SUVavg in normal brain.

2.3. Fusion Imaging with FRP170 and MET

Before assessments using fusion images superimposing FRP170 with MET, we roughly observed the distributions of uptake areas on color images of FRP170 scan and MET scan. We then assessed distributions of uptake for FRP170 and MET using extracted pixels on superimposed images. We extracted those pixels within the tumor on MET image that showed between the SUV at T/N ratio ≥1.6 and SUVmax. This threshold was based on previous reports that active glioma can be differentiated from areas such as normal tissue and radiation necrosis using a T/N cut-off of 1.5 - 1.6 [14] [15] [16]. We then also extracted those pixels on FRP170 PET image that showed between the SUV at T/N ratios above various thresholds and SUVmax. We changed T/N cut-off value in increments of 0.1 between SUVmin and SUVmax in the tumor on FRP170 scan, and extracted pixels between the SUV at each changed T/N cut-off value and SUVmax within the tumor for each patient. All data sets of extracted pixels were transferred to available software for display for multimodal medical images (Analyze version 11.0; AnalyzeDirect, Overland Park, KS). Pixels extracted from each FRP170 or MET image were automatically transformed into the template of standard brain size and shape which was set in the software, and were finally superimposed on an image. On each superimposed image, we determined whether FRP170-accumulating extracted pixels showing SUV above the threshold set according to the T/N could be separated from MET-accumulating extracted pixels.

3. Results

We satisfactorily performed both PET scans with FRP170 and MET in all patients. On color mapping without any threshold, high uptake areas on FRP170 PET and MET PET seemed distributed at nearly the same regions. **Table 1** provides data on SUVmin and SUVmax in tumor and SUVavg in normal tissue for the extraction of pixels from FRP170 PET and SUVmax in tumor and SUVavg in normal tissue for the extraction of pixels from MET PET in each patient. Procedures for pixel extraction vividly demonstrated distributions of high accumulation with FRP170 and MET. In a case, both of reddish-colored pixels indicating high uptake areas on MET image (**Figure 1(a)**) and FRP170 image (**Figure 1(b)**) were seen at the nearly same region of the outside of tumor. Also in another case, high uptake areas of both PET images were revealed at the nearly same region of the inside of tumor (**Figure 1(e)**, **Figure 1(f)**). When setting a T/N resulting in a threshold SUV equivalent to SUVmin in the tumor, *i.e.*, extracting pixels between SUVmin and SUVmax, extracted pixels were depicted as the entire tumor bulk in all patients. For instance, we realized that extracted pixels between SUVmin of 1.59 and SUVmax of 2.20 showed the same feature as the tumor which was depicted on Gd-T1WI in Case 3 (**Figure 1(c)**, **Figure 1(d)**). Also in Case 4, extracted pixels with SUV between 1.47 as SUVmin and 1.92 as SUVmax were distributed at the areas where were shown as enhanced regions on

Gd-T1WI (Figure 1(g), Figure 1(h)).

For procedures of superimposed imaging, pixels showing T/N ratio more than 1.6 were extracted from MET-PET images (left line in Figure 2 for Case 3; left line in Figure 3 for Case 4). For FRP170 image, the threshold for the extraction of pixels was changed in increments of 0.1 from T/N at SUVmin to T/N at SUVmax in the tumor (right lines in Figure 2, Figure 3). On fusion images superimposing pixels extracted from FRP170 image on those extracted from MET image (middle lines in Figure 2, Figure 3), fusion imaging at thresholds near the SUVmin showed that overlapping distributions between the two tracers certainly existed within the tumor in all patients (the top rows in Figure 2, Figure 3). The more the threshold was raised from T/N at SUVmin to that at SUVmax, the less

Table 1. All data for extraction of pixels from FRP170 PET and MET PET.

No	FRP170				MET		
	SUVmin (T)/SUVavg (N)	T/N	SUVmax (T)/SUVavg (N)	T/N	SUVmax (T)	SUVavg (N)	SUV (T) at T/N = 1.6
1	1665/737	2.26	1818/737	2.47	3018	1007	1611
2	1046/721	1.45	1630/721	2.26	6309	1833	2933
3	1586/1253	1.27	2157/1253	1.72	5044	1409	2254
4	1470/596	2.56	1916/596	3.21	5654	1389	2222
5	1209/1209	1.00	1923/1209	1.59	2913	1057	1691
6	2165/1600	1.35	3125/1600	1.95	5949	1148	1837
7	2066/2065	1.00	2770/2065	1.34	6702	1487	2679
8	1637/1354	1.27	2137/1354	1.58	3199	1232	1971

T, tumor; N, normal brain; T/N, ratio of SUV in tumor divided by SUVavg in apparently normal brain.

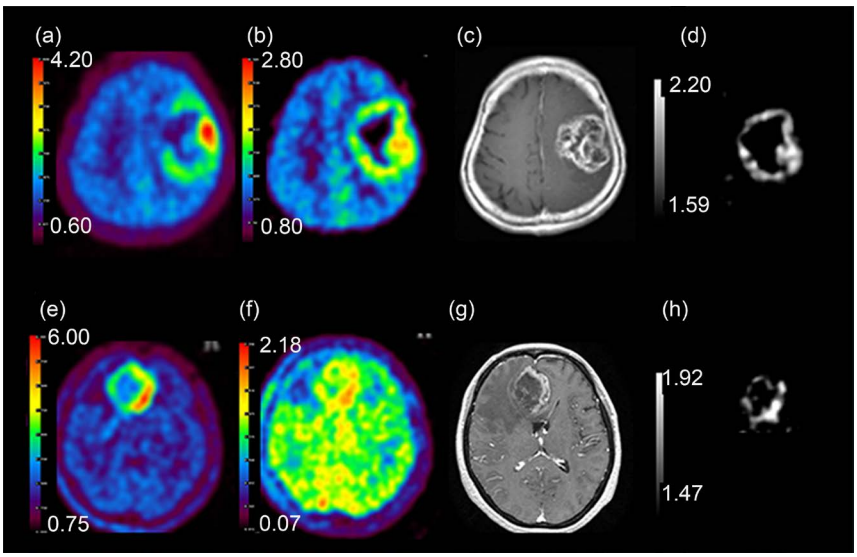

Figure 1. Representative images for Case 3 (a) (d), and Case 4 (e)-(h) in **Table 1**. (a) (e) MET PET; (b) (f) FRP170 PET; (c) (g) gadolinium-enhanced T1-weighted magnetic resonance imaging; (d) (h) extracted pixels between SUVmin and SUVmax in tumor.

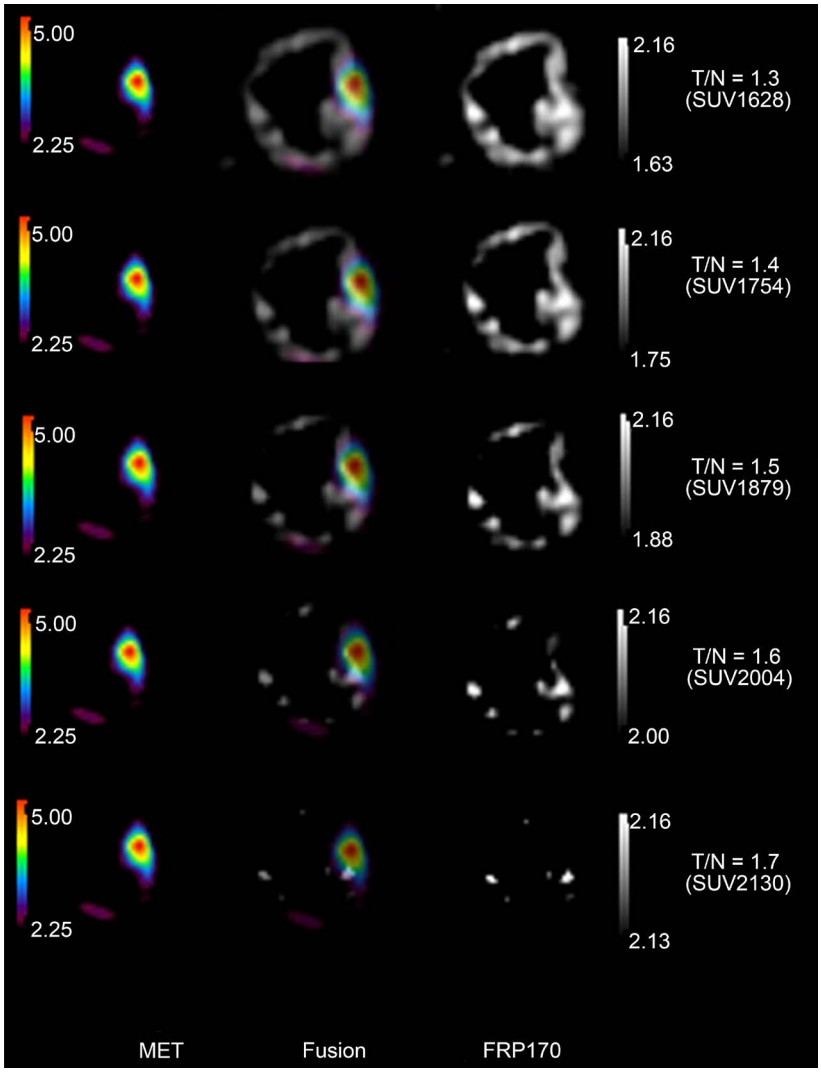

Figure 2. Representative fusion imaging superimposing pixels extracted from FRP170 PET on those extracted from MET PET in Case 3. Left, pixels extracted from MET; middle, fusion imaging; right, pixels extracted from FRP170. T/N and SUV values show the lower limit in the extraction range.

the area of pixels extracted from FRP170 image overlapped in all patients (from the top rows to the lowest rows in **Figure 2**, **Figure 3**). Pixels extracted from FRP170 image at a T/N ratio close to the SUVmax were extremely shrunken, but partially overlapped on the edge of pixel areas extracted from MET PET (the lowest rows in **Figure 2**, **Figure 3**). In that situation, however, these overlapping regions did not involve regions of high MET accumulation shown as reddish areas on MET image. Thus, pixels extracted from FRP170 PET at all thresholds could not avoid partial overlap with pixels extracted from MET PET in all patients.

4. Discussion

Cell hypoxia results from demand for and consumption of oxygen greatly exceeding the supply due to chaotic proliferation within the tumor. The relationship

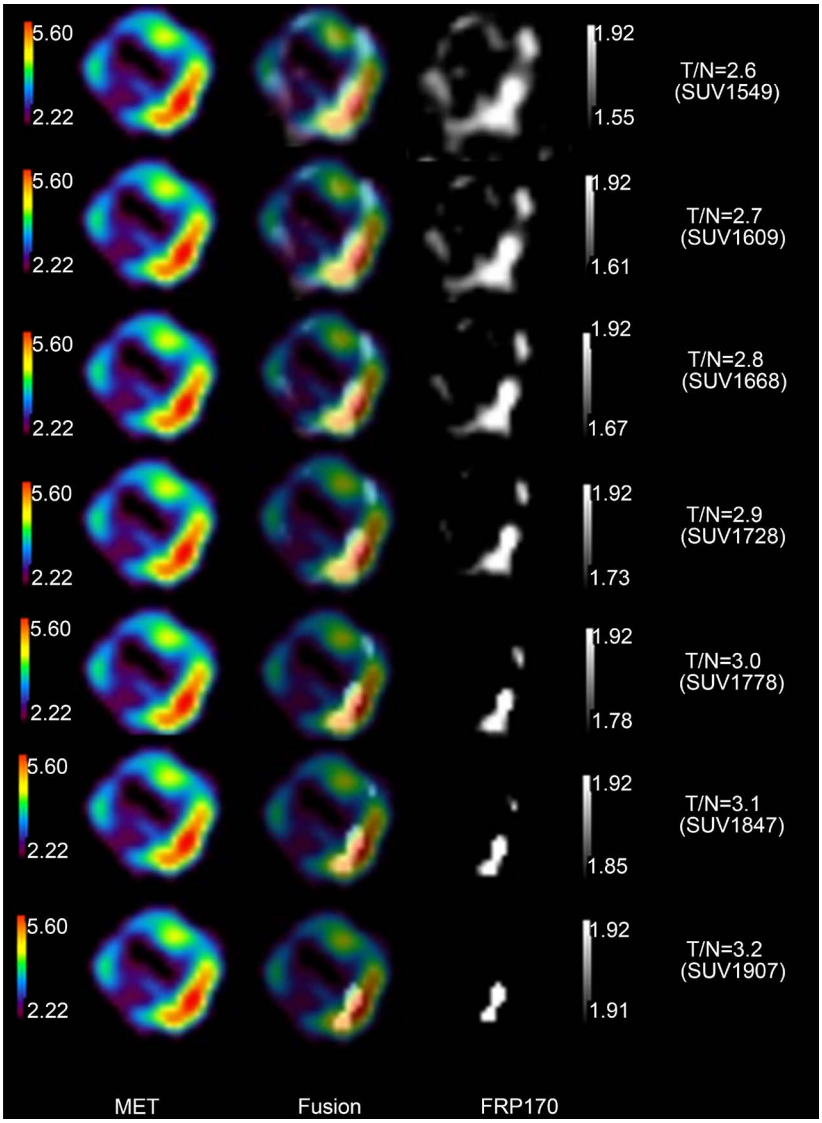

Figure 3. Representative fusion imaging superimposing pixels extracted from FRP170 PET on those extracted from MET PET in Case 4. Left, pixels extracted from MET; middle, fusion imaging; right, pixels extracted from FRP170. T/N and SUV values show the lower limit in the extraction range.

between hypoxia and proliferation was thus generally expected to be an inverse correlation. Indeed, an immunohistochemically locoregional observation demonstrated an inverse distribution of immunohistochemically stained cells between EF-5 as a hypoxia marker and Ki-67 as a proliferation marker [7]. Conversely, previous studies using immunohistochemical staining with Ki-67 have shown that hypoxic tissues with high accumulation of FRP170 or FMISO retained high proliferation in a rat model of glioma *in vitro* [11], and glioblastoma [9] and lung cancer [10] *in vivo*. In the present study, simple comparisons of uptake areas between FRP170 and MET showed similarly consistent regions within the tumor. Furthermore, pixels extracted using a T/N resulting in a threshold SUV above the SUVmin from FRP170 PET were depicted in the entire tumor. These findings indicated that no considerations of threshold for uptake

of FRP170 will certainly contribute to the inclusion of proliferating areas within FRP170 uptake areas.

As mentioned above, some reports documented that tissues obtained from high-uptake areas on PET image with the hypoxic radiotracer can include regions retaining proliferative activity. In those reports, however, uptake areas on FRP170 image were not detected by any terms or threshold. Therefore, a possibility that obtained tissues included not only densely packed hypoxic cells but also loosely packed hypoxic cells was not denied. That was why we tried to evaluate overlapping pixels from FRP170 and MET images at the threshold for extraction of FRP170-accumulating pixels of near SUVmax, where should represent the condition of densely packed hypoxic cells. To the best our knowledge, no previous reports have documented attempts to depict densely populated hypoxic cells without proliferation activity on either FRP170 PET or FMISO PET. High SUV on FRP170 PET should indicate densely populated hypoxic cells without high proliferation activity, since the relationship between extents of hypoxia and proliferation in cancer tissues shows an inverse gradient between mild and severe degrees. In this study, we changed the T/N to determine the threshold for extracting pixels on FRP170 PET. As a result, we found that pixels extracted using a T/N resulting in an SUV near SUVmax in tumor from FRP170 PET were scarcely separated from pixels (reddish-colored areas) suggesting high proliferation from MET PET. However, FRP170-extracted pixels at all thresholds could not be completely separated from extracted pixels representing actively proliferating cells on MET PET. The finding that uptake areas of FRP170 PET necessarily include proliferation lesions means that close attention should be paid to interpretations of findings on FRP170 PET.

The reasons why FRP170-uptake lesions necessarily retain proliferative potential have not been clarified, but might result from biological limitations to the accumulation of FRP170 in cells. The range of oxygen concentrations under which FRP170 accumulates in cells has remained unclear, but accumulation of FMISO in cells has been reported to increase under hypoxia with O_2 at less than 10 mmHg [17]. FRP170 could be considered to increase accumulation under the same conditions as FMISO, because FRP170 is synthesized from the 2-nitroimidazole derivative in common with FMISO. Given that the range of hypoxia in glioblastoma has been recognized as 4 ~ 20 mmHg in mild hypoxia and 0.75 ~ 4 mmHg in moderate/severe hypoxia [18], FRP170 could not be detected in cells only under moderate or severe hypoxia, but also in cells under mild hypoxia. An experimental study reported that a mean oxygen pressure within glioblastoma tissues corresponding to high-uptake areas on FRP170 image was 21.7 mmHg [4]. Although the figure in that report was beyond the range of mild hypoxia described above, FRP170 might be able to accumulate in cells under oxygen pressure of mild hypoxia at the least. Another reason may be that FRP170 cannot accumulate in cells falling almost undergoing necrosis or apoptosis, but only in viable cells capable of the complicated metabolism that can make FRP170 bind to intracellular structures [6] [9] [19] [20]. These terms

should lead to sustained proliferative activity in areas with accumulation of FRP170.

Some limitations regarding the study results must be considered. First, the sample size in this study was small, because relatively few patients met the inclusion criteria for the study. Although we believe the results represent the coexistence of cells accumulating FRP170 and MET, additional investigations with a larger number of patients might be needed. Second, we did not change the threshold for extracting pixels from MET PET like FRP170 PET, but just set the T/N as 1.6. However, the aim of this study was to clarify whether FRP170 PET could detect densely populated hypoxic areas without proliferative potential, when FRP170 PET alone would be performed. Third, we did not observe histological findings using specimens obtained from regions accumulating with both tracers or showing mainly either tracer alone. The lack of pathological investigations also meant that the practical extent of oxygen pressure at the various thresholds remained unclear. The finding that high-uptake area accumulating with FRP170, where consisted of densely packed hypoxic cells, can contain proliferating cells accumulating with MET in the current study implies an existence of cells retaining proliferating potential under hypoxia. To clarify this implication, a histochemical study such as a double-immunostaining with both proliferation and hypoxia markers is needed. These issues should be clarified in future studies.

5. Conclusion

To clarify whether FRP170 image can detect densely populated hypoxic areas without proliferating potential in glioblastoma, we assessed distribution of pixels accumulating with FRP170 and MET on superimposing of both tracer images in eight patients. As a result, pixels with FRP170 could not be completely separated from pixels with MET in all patients, even pixels with FRP170 showing almost maximum SUV. The current study supported the possibility that high-uptake areas on FRP170 PET can retain proliferative activity.

Acknowledgements

This study was supported in part by Grant-in-Aid for JSPS KAKENHI (Grant no. 26462764) and a Strategic Medical Science Research (Grant no. S1491001) from the Ministry of Education, Culture, Sports, Science and Technology of Japan.

References

[1] Mendichovszky, I. and Jackson, A. (2011) Imaging Hypoxia in Gliomas. *The British Journal of Radiology*, **84**, S145-S158. https://doi.org/10.1259/bjr/82292521

[2] Kawai, N., Maeda, Y., Kudomi, N., *et al.* (2011) Correlation of Biological Aggressiveness Assessed by 11C-Methionine PET and Hypoxic Burden Assessed by 18F-Fluoromisonidazole PET in Newly Diagnosed Glioblastoma. *European Journal of Nuclear Medicine and Molecular Imaging*, **38**, 441-450. https://doi.org/10.1007/s00259-010-1645-4

[3] Swanson, K.R., Chakraborty, G., Wang, C.H., *et al.* (2009) Complementary but Distinct Roles for MRI and 18F-Fluoromisonidazole PET in the Assessment of Human Glioblastomas. *Journal of Nuclear Medicine*, **50**, 36-44. https://doi.org/10.2967/jnumed.108.055467

[4] Beppu, T., Terasaki, K., Sasaki, T., *et al.* (2014) Standardized Uptake Value in High Uptake Area on Positron Emission Tomography with (18)F-FRP170 as a Hypoxic Cell Tracer Correlates with Intratumoral Oxygen Pressure in Glioblastoma. *Molecular Imaging and Biology*: *MIB*: *the Official Publication of the Academy of Molecular Imaging*, **16**, 127-135. https://doi.org/10.1007/s11307-013-0670-7

[5] Shibahara, I., Kumabe, T., Kanamori, M., *et al.* (2010) Imaging of Hypoxic Lesions in Patients with Gliomas by Using Positron Emission Tomography with 1-(2-[18F] Fluoro-1-[Hydroxymethyl]Ethoxy)Methyl-2-Nitroimidazole, a New 18F-Labeled 2-Nitroimidazole Analog. *Journal of neurosurgery*, **113**, 358-368. https://doi.org/10.3171/2009.10.JNS09510

[6] Kaneta, T., Takai, Y., Iwata, R., *et al.* (2007) Initial Evaluation of Dynamic Human Imaging Using 18F-FRP170 as a New PET Tracer for Imaging Hypoxia. *Annals of Nuclear Medicine*, **21**, 101-107. https://doi.org/10.1007/BF03033987

[7] Evans, S.M., Jenkins, K.W., Chen, H.I., *et al.* (2010) The Relationship among Hypoxia, Proliferation, and Outcome in Patients with De Novo Glioblastoma: A Pilot Study. *Translational Oncology*, **3**, 160-169. https://doi.org/10.1593/tlo.09265

[8] Tanaka, T., Furukawa, T., Fujieda, S., Kasamatsu, S., Yonekura, Y. and Fujibayashi, Y. (2006) Double-Tracer Autoradiography with Cu-ATSM/FDG and Immunohistochemical Interpretation in Four Different Mouse Implanted Tumor Models. *Nuclear Medicine and Biology*, **33**, 743-750. https://doi.org/10.1016/j.nucmedbio.2006.05.005

[9] Beppu, T., Sasaki, T., Terasaki, K., *et al.* (2015) High-Uptake Areas on Positron Emission Tomography with the Hypoxic Radiotracer (18)F-FRP170 in Glioblastomas Include Regions Retaining Proliferative Activity under Hypoxia. *Annals of Nuclear Medicine*, **29**, 336-341. https://doi.org/10.1007/s12149-015-0951-0

[10] Cherk, M.H., Foo, S.S., Poon, A.M., *et al.* (2006) Lack of Correlation of Hypoxic Cell Fraction and Angiogenesis with Glucose Metabolic Rate in Non-Small Cell Lung Cancer Assessed by 18F-Fluoromisonidazole and 18F-FDG PET. *Journal of Nuclear Medicine*, **47**, 1921-1926.

[11] Hatano, T., Zhao, S., Zhao, Y., *et al.* (2013) Biological Characteristics of Intratumoral [F-18]Fluoromisonidazole Distribution in a Rodent Model of Glioma. *International Journal of Oncology*, **42**, 823-830.

[12] Ishikawa, Y., Iwata, R., Furumoto, S. and Takai, Y. (2005) Automated Preparation of Hypoxic Cell Marker [18F]FRP-170 by On-Column Hydrolysis. *Applied Radiation and Isotopes*, **62**, 705-710.

[13] Pascali, C.B.A., Iwata, R., Decise, D., Crippa, F. and Bombardieri, E. (1999) High Efficiency Preparation of [11C]Methionine by On-Column [11C]Methylation on C18 Sep-Pak. *Journal of Labelled Compounds and Radiopharmaceuticals*, **42**, 715-724. https://doi.org/10.1002/(SICI)1099-1344(199908)42:8<715::AID-JLCR224>3.0.CO;2-3

[14] Galldiks, N., Kracht, L.W., Burghaus, L., *et al.* (2006) Use of 11C-Methionine PET to Monitor the Effects of Temozolomide Chemotherapy in Malignant Gliomas. Eur *Journal of Nuclear Medicine and Molecular Imaging*, **33**, 516-524. https://doi.org/10.1007/s00259-005-0002-5

[15] Herholz, K., Holzer, T., Bauer, B., *et al.* (1998) 11C-Methionine PET for Differential

Diagnosis of Low-Grade Gliomas. *Neurology*, **50**, 1316-1322. https://doi.org/10.1212/WNL.50.5.1316

[16] Terakawa, Y., Tsuyuguchi, N., Iwai, Y., *et al.* (2008) Diagnostic Accuracy of 11C-Methionine PET for Differentiation of Recurrent Brain Tumors from Radiation Necrosis after Radiotherapy. *Journal of Nuclear Medicine*, **49**, 694-699. https://doi.org/10.2967/jnumed.107.048082

[17] Rasey, J.S., Hofstrand, P.D., Chin, L.K. and Tewson, T.J. (1999) Characterization of [18F]Fluoroetanidazole, a New Radiopharmaceutical for Detecting Tumor Hypoxia. *Journal of Nuclear Medicine*, **40**, 1072-1079.

[18] Evans, S.M., Jenkins, K.W., Jenkins, W.T., *et al.* (2008) Imaging and Analytical Methods as Applied to the Evaluation of Vasculature and Hypoxia in Human Brain Tumors. *Radiation Research*, **170**, 677-690. https://doi.org/10.1667/RR1207.1

[19] Kaneta, T., Takai, Y., Kagaya, Y., *et al.* (2002) Imaging of Ischemic but Viable Myocardium Using a New 18F-Labeled 2-Nitroimidazole Analog, 18F-FRP170. *Journal of Nuclear Medicine*, **43**, 109-116.

[20] Krohn, K.A., Link, J.M. and Mason, R.P. (2008) Molecular Imaging of Hypoxia. *Journal of Nuclear Medicine*, **49**, 129S-148S. https://doi.org/10.2967/jnumed.107.045914